

Experimental realization of the quantum universal NOT gate

F. De Martini*, V. Bužek†‡, F. Sciarrino* & C. Sias*

* Dipartimento di Fisica and Istituto Nazionale di Fisica della Materia, Università “La Sapienza”, 00185 Roma, Italy

† Research Center for Quantum Information, Institute of Physics, Slovak Academy of Sciences, Dúbravská cesta 9, 842 28 Bratislava, Slovakia

‡ Department of Mathematical Physics, National University of Ireland, Maynooth, Ireland

In classical computation, a ‘bit’ of information can be flipped (that is, changed in value from zero to one and vice versa) using a logical NOT gate; but the quantum analogue of this process is much more complicated. A quantum bit (qubit) can exist simultaneously in a superposition of two logical states with complex amplitudes, and it is impossible^{1–3} to find a universal transformation that would flip the original superposed state into a perpendicular state for all values of the amplitudes. But although perfect flipping of a qubit prepared in an arbitrary state (a universal NOT operation) is prohibited by the rules of quantum mechanics, there exists an optimal approximation² to this procedure. Here we report the experimental realization of a universal quantum machine⁴ that performs the best possible approximation to the universal NOT transformation. The system adopted was an optical parametric amplifier of entangled photon states, which also enabled us to investigate universal quantum cloning.

In order to understand the problem of spin flipping, we consider the Poincaré sphere, which represents a state space of a qubit. The points corresponding to $|\Psi\rangle$ and $|\Psi^\perp\rangle$ are antipodes. The desired

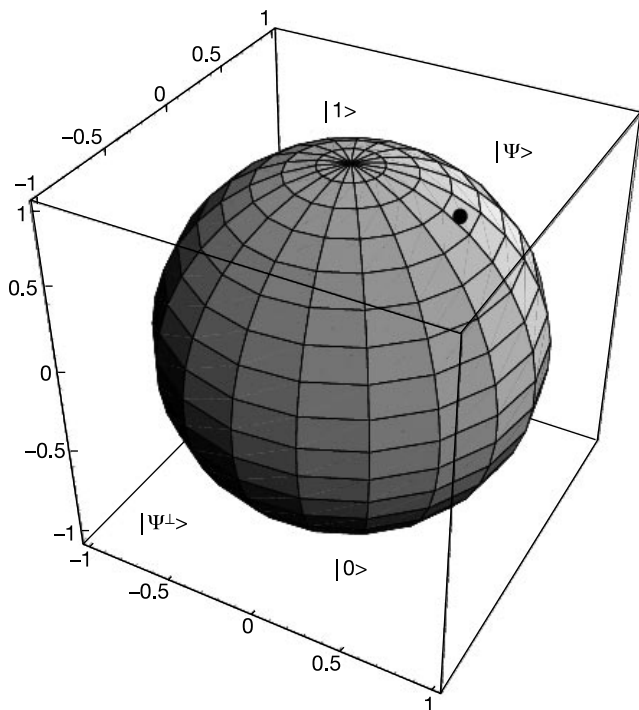


Figure 1 The state space of a qubit is a Poincaré sphere. Pure states are represented by points on the sphere, while statistical mixtures are points inside the sphere. The universal NOT operation corresponds to the inversion of the sphere, because the states $|\Psi\rangle$ and $|\Psi^\perp\rangle$ are antipodes.

spin-flip operation is therefore the inversion of the Poincaré sphere (Fig. 1). It is known that this inversion preserves angles. Therefore, by the arguments of the Wigner theorem the ideal spin-flip operation must be implemented either by a unitary or by an anti-unitary operation. Unitary operations correspond to proper rotations of the Poincaré sphere, whereas anti-unitary operations correspond to orthogonal transformations with determinant equal to -1 . The spin-flip is an anti-unitary operation—that is, it is not completely positive. It is exactly this property that makes the spin-flip operation so important in all criteria of inseparability for two-qubit systems. On the other hand, from above it follows that in the unitary world the ideal universal (U) NOT gate, which would flip a qubit in an arbitrary state, does not exist.

As it is not possible to realize a perfect U-NOT gate which would flip an arbitrary qubit state, it is necessary to investigate what is the best approximation to this gate. This investigation illuminates bounds on information processing imposed by rules of quantum mechanics. There are two possible approaches. The first is based on the measurement of input qubit(s). By using the results of an optimal measurement, one can manufacture an orthogonal qubit, or any desired number of them. In this case, the ‘fidelity’ (F) of the NOT operation is equal to the fidelity of estimation of the state of the input qubit(s). The second approach would be to approximate an anti-unitary transformation on a Hilbert space of the input qubit(s) by a unitary transformation on a larger Hilbert space which describes the input qubit(s) and ancillas².

The best achievable fidelity of both flipping approaches is the same^{2,3}. That is, the fidelity of the optimal U-NOT gate is equal to the fidelity of the best state-estimation performed on input qubits⁵ (one might say, that in order to flip a qubit we have to transform it into a bit). Even though the fidelity of both processes is the same, the U-NOT gate has a great advantage. Namely, in the measurement-based approach the information encoded in a state of a qubit is irreversibly lost by the measurement process, whereas in the U-NOT gate the information is only redistributed according to specific rules, but owing to the unitarity of the gate it can be recovered.

In our experiment (see below, and Methods) we will consider a flipping of a single qubit. The optimal U-NOT transformation reads²:

$$\hat{U}|\Psi\rangle_a \otimes |X\rangle_{bc} = (2/3)^{1/2} |\Psi\Psi\rangle_{ab} |\Psi^\perp\rangle_c - (1/3)^{1/2} \{|\Psi, \Psi^\perp\rangle\}_{ab} |\Psi\rangle_c \quad (1)$$

where the gate is always prepared in some state $|X\rangle_{bc}$, independently of the input state $|\Psi\rangle$, and $\{|\Psi, \Psi^\perp\rangle\}$ is a symmetric state of two orthogonal qubits. To be specific, equation (1) describes a process

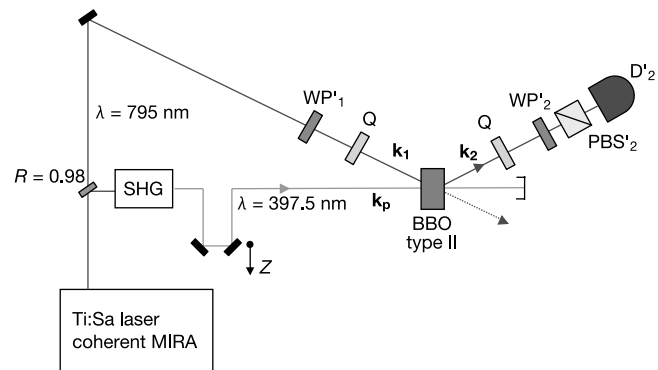


Figure 2 Layout of the apparatus used for the experimental verification of the universality of the optical parametric amplifier (OPA). Various polarization (π)-states of the injected pulse were prepared by a wave-plate WP_1 (either $\lambda/2$ or $\lambda/4$) inserted on the injection mode k_1 . See Methods for details.

when the original qubit is encoded in system a while the flipped qubit is in system c . The density operator describing the output state of system c is:

$$\sigma^{(\text{out})} = 1/3|\Psi^\perp\rangle\langle\Psi^\perp| + 1/3\mathbf{1} = 2/3|\Psi^\perp\rangle\langle\Psi^\perp| + 1/3|\Psi\rangle\langle\Psi| \quad (2)$$

The identity operator $\mathbf{1}$ in equation (2) reflects the amount of noise induced by the U-NOT gate. The average fidelity of the universal NOT gate is $F = \langle\Psi^\perp|\sigma^{(\text{out})}|\Psi^\perp\rangle = 2/3$. The discussion above describes the case of a single input qubit. When generally N qubits are considered at the input of the U-NOT gate, then the fidelity depends on the number N of input qubits prepared in the state $|\Psi\rangle$. The larger their number, the larger is the fidelity. Specifically, we find that the explicit expression for the fidelity of the U-NOT is $F = (N + 1)/(N + 2)$, which is exactly the same as the fidelity of the optimal state estimation⁵. We see that in the quantum world governed by unitary operations anti-unitary operations can be performed with a fidelity which is bounded by the amount of classical information available about states of quantum systems.

A natural way to encode a qubit into a physical system is to utilize the polarization states of the photon. In this case, the U-NOT gate can be realized via stimulated emission. The central idea of our experiment is based on the proposal that universal quantum machines⁴ such as the quantum cloner can be realized with the help of stimulated emission in parametric downconversion⁶⁻⁸. Specifically, we consider a qubit to be encoded in a polarization state of a single photon. This photon was injected as the input state into an optical parametric amplifier (OPA) excited by a pulsed, mode-locked ultraviolet (UV) laser beam⁶. The relevant modes of the nonlinear (NL) three-wave interaction driven by the UV pulse were the spatial modes with wavevectors \mathbf{k}_1 and \mathbf{k}_2 each supporting a horizontal (H) and a vertical (V) linear-polarization (π) of the interacting photons: for example, π_{1H} is the horizontal polarization unit vector associated with \mathbf{k}_1 . The OPA was frequency degenerate: that is, the interacting photons had the same wavelength $\lambda = 795$ nm. More experimental details are given in Methods. The action of the OPA under suitable conditions, realized in

our case, is described by the ‘squeezing’ hamiltonian⁶: $H_{\text{int}} = i\hbar\chi(\hat{a}_H^\dagger\hat{b}_V^\dagger - \hat{a}_V^\dagger\hat{b}_H^\dagger) + \text{h.c.}$, where χ expresses the nonlinear susceptibility of the active crystal, and h.c. is the hermitian conjugate. Here the field operators \hat{a} and \hat{b} are assumed to be acting on modes \mathbf{k}_1 and \mathbf{k}_2 , respectively. It has been recently shown by theory^{7,8} that H_{int} is invariant under simultaneous general SU(2) transformations of the polarization vectors for modes \mathbf{k}_1 and \mathbf{k}_2 . We may then cast the expression above in the following form:

$$H_{\text{int}} = i\hbar\chi(\hat{a}_\pi^\dagger\hat{b}_{\pi^\perp}^\dagger - \hat{a}_{\pi^\perp}^\dagger\hat{b}_\pi^\dagger) + \text{h.c.} \quad (3)$$

where the field labels refer to the two mutually orthogonal polarization unit vectors for each mode, π and π^\perp , corresponding respectively to the state vectors: $|\Psi\rangle$ and $|\Psi^\perp\rangle$.

Equation (3) is of central importance in the context of the present work as the amplification efficiency of this type of OPA under any externally injected quantum field (consisting, for example, of a single photon or of a classical ‘coherent’ field) can be made independent of the polarization state of the field. Indeed, it has been shown by a recent experiment on ‘universal quantum cloning’⁹ that the OPA ‘gain’ $g = \chi t$ (where t is time) is independent of any (unknown) polarization state of the injected field: this precisely represents the necessary universality (U) property of the U-NOT gate. We assume that the input photon in the mode \mathbf{k}_1 has a polarization π , a condition expressed by the state vector $|\Psi\rangle$, as said. We will describe this polarization state as $\hat{a}_\pi^\dagger|0, 0\rangle_{\mathbf{k}_1} = |1, 0\rangle_{\mathbf{k}_1}$ where we have used notation introduced in ref. 7: that is, the state $|m, n\rangle_{\mathbf{k}_1}$ represents a state with m photons of the mode \mathbf{k}_1 having the polarization π , while n photons have the polarization π^\perp . Initially there are no excitations in the mode \mathbf{k}_2 . The initial polarization state of these two modes reads $|1, 0\rangle_{\mathbf{k}_1} \otimes |0, 0\rangle_{\mathbf{k}_2}$ and it evolves according to the unitary operator $\hat{U} \equiv \exp(-iH_{\text{int}}t/\hbar)$:

$$\hat{U} |1, 0\rangle_{\mathbf{k}_1} \otimes |0, 0\rangle_{\mathbf{k}_2} = |1, 0\rangle_{\mathbf{k}_1} \otimes |0, 0\rangle_{\mathbf{k}_2} + g(2^{1/2}|2, 0\rangle_{\mathbf{k}_1} \otimes |0, 1\rangle_{\mathbf{k}_2} - |1, 1\rangle_{\mathbf{k}_1} \otimes |1, 0\rangle_{\mathbf{k}_2}) \quad (4)$$

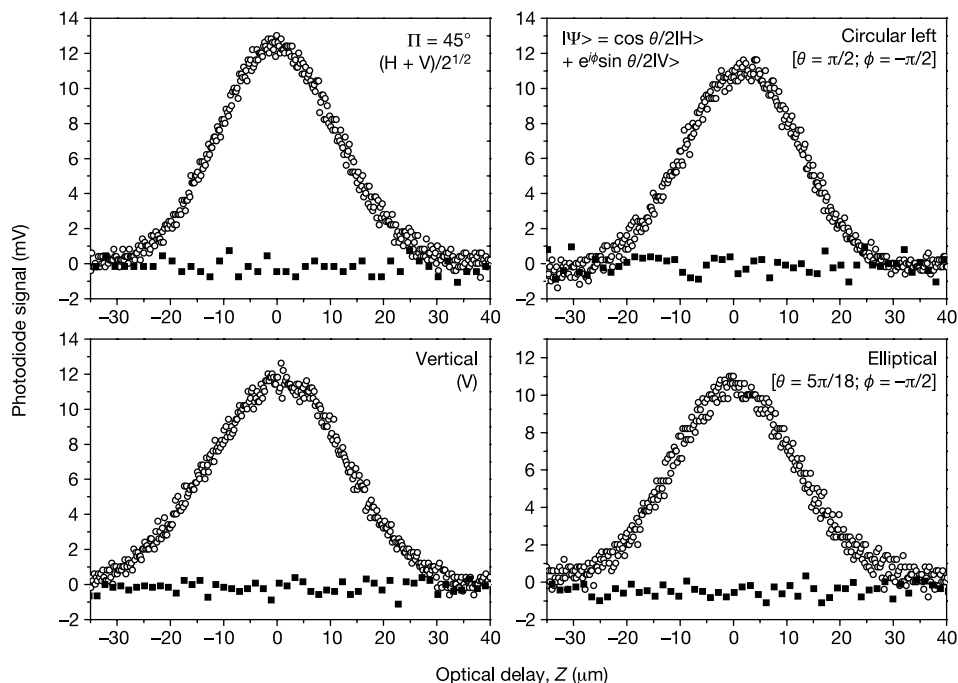


Figure 3 Experimental verification of the universality of the OPA system for different field polarizations, either linear (Π), circular, or generally elliptical. The plots show the amplification pulses detected by D_2 on the OPA output mode, \mathbf{k}_2 , under the injection on the input mode \mathbf{k}_1 of attenuated laser coherent pulses. Each plot corresponds to a state of

definite input polarization π : $\cos(\theta/2)|H\rangle + e^{i\phi}\sin(\theta/2)|V\rangle$ (see text for details). The lack of amplification by detection on the ‘wrong’ polarization channel on mode \mathbf{k}_2 is shown by the filled squares.

This approximation for the state vector describing the two modes at times $t > 0$ is sufficient, because the value of g is usually very small in our experiment (see below): $g \ll 1$. The zero-order term corresponds to the process when the input photon in the mode \mathbf{k}_1 did not interact in the nonlinear medium, while the second term describes the first-order amplification process. This second term is formally equal (up to a normalization factor) to the right-hand side of equation (2). Here the state $|2,0\rangle_{\mathbf{k}_1}$ describing two photons of the mode \mathbf{k}_1 in the polarization state π corresponds to the state $|\Psi\Psi\rangle$. This state vector describes the cloning of the original photon⁷⁻⁹. The vector $|0,1\rangle_{\mathbf{k}_2}$ describes the state of the mode \mathbf{k}_2 with a single photon with the polarization orthogonal to π . That is, the output state vector $|\Psi^\perp\rangle = |0,1\rangle_{\mathbf{k}_2}$ represents the flipped version of the input $|\Psi\rangle = |1,0\rangle_{\mathbf{k}_1}$.

To see that the stimulated emission is responsible for creation of the flipped qubit, we compare the state represented by equation (4) with the output state when the vacuum is injected into the NL crystal. In this case, to the same order of approximation as above, we obtain:

$$\hat{U}|0,0\rangle_{\mathbf{k}_1} \otimes |0,0\rangle_{\mathbf{k}_2} = |0,0\rangle_{\mathbf{k}_1} \otimes |0,0\rangle_{\mathbf{k}_2} + g(|1,0\rangle_{\mathbf{k}_1} \otimes |0,1\rangle_{\mathbf{k}_2} - |0,1\rangle_{\mathbf{k}_1} \otimes |1,0\rangle_{\mathbf{k}_2}) \quad (5)$$

We see that the flipped qubit described by the state vector $|0,1\rangle_{\mathbf{k}_2}$ in the right-hand sides of equations (4) and (5) appears with different amplitudes corresponding to the ratio of the probabilities being $R = 2:1$. Our experiment indeed consists of the measurement of R , as we shall see. Note also that the U-NOT operation is not altered by multiplying H_{int} by any overall phase factor.

On the ‘microscopic’ quantum level, the justification of this U property of the OPA amplifier resides in the SU(2) invariance of H_{int} when the spatial orientation of the OPA crystal makes it available for creation by spontaneous parametric downconversion (SPDC) of two-photon entangled ‘singlet’ states^{7,8}. But we note that in the present context the universality property (that is, the π -insensitivity of g) is indeed a ‘macroscopic’ classical feature of the OPA device. So it can be tested equally well by injection of either a quasi-classical radiation state (for example, a coherent field), or of a quantum radiation state (for example, a single-photon Fock state). The test corresponding to injection of an attenuated coherent field is shown in Figs 2 and 3. Details of the apparatus (Fig. 2) are given below.

The universality condition is demonstrated by the plots of Fig. 3 showing the amplification pulses detected by D_2' on the OPA output mode \mathbf{k}_2 . Each plot corresponds to a definite state of polarization (π) of the field injected on mode \mathbf{k}_1 : $[\cos(\theta/2)|H\rangle + e^{i\phi}\sin(\theta/2)|V\rangle]$. The polarization was either linear (that is, $\theta = \pi/2, \pi; \phi = 0$), or circular (that is, $\theta = \pi/2; \phi = -\pi/2$), or very generally elliptical: $\theta = 5\pi/18; \phi = -\pi/2$. We may check that, in

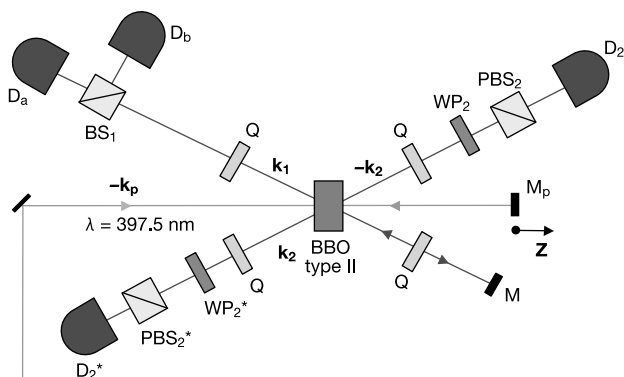


Figure 4 Experimental realization of the U-NOT gate. A single photon, $N = 1$, was injected with a definite π -state into the NL crystal of the OPA along the mode \mathbf{k}_1 . The π flipping effect was detected on mode \mathbf{k}_2 . See Methods for details.

spite of the different input π -states, the amplification curves are almost identical. Each coherent pulse injected on the mode \mathbf{k}_1 was amplified into an average photon number $M' \approx 5 \times 10^3$ on the output mode \mathbf{k}_2 .

We now consider the U-NOT gate. By virtue of the tested universality of the OPA amplification, it is sufficient to consider here the OPA injection on mode \mathbf{k}_1 by a single photon in just one π -state; for example, in the horizontal π -state: $|\Psi\rangle = |H\rangle$ (Fig. 4).

From the analysis above, it follows that the state of the field emitted by the OPA indeed realizes the U-NOT gate operation: that is, the ‘optimal’ realization of the transformation by flipping of the original qubit originally encoded in the mode \mathbf{k}_1 . The flipped qubit at the output is in the mode \mathbf{k}_2 . As shown earlier, the state created by the U-NOT gate cannot be a pure one. There is a minimal amount of noise induced by the process of flipping, which is inevitable in order to preserve complete positiveness of the U-NOT gate. This mixed state is described by the density operator, equation (2). The polarization state of the output photon in the mode \mathbf{k}_2 in our experiment is indeed described by this density operator.

The plots of Fig. 5 report our experimental four-coincidence data as function of the time superposition of the UV pump and of the injected single-photon pulses. Our main result consists of the determination of the ratio R between the height of the central peak and that of the flat ‘noise’ contribution. To understand this ratio, we first note that the most efficient stimulation process in the OPA is achieved when a perfect match is achieved: that is, time and space overlap between the UV pump pulse and the optical pulse carrying the input photon. This situation corresponds to the value of the mirror position Z equal to zero. As soon as the mirror is displaced from the position $Z = 0$, the time overlap of the two interacting optical pulses decreases, and the stimulation becomes increasingly less efficient—that is, the spin-flip operation is more noisy. In the limit of large displacements Z , the spin flipping is totally random owing to the fact that the process corresponds to injecting the vacuum field into the crystal. The theoretical ratio between the corresponding probabilities is $R = 2$, as mentioned earlier. In the experiment we have found this ratio to be $R = 1.70 \pm 0.06$. This corresponds, by virtue of equations (4) and (5) above, to a measured value of the fidelity of the U-NOT device: $F = R/(R + 1) = 0.630 \pm 0.008$, to be compared with the theoret-

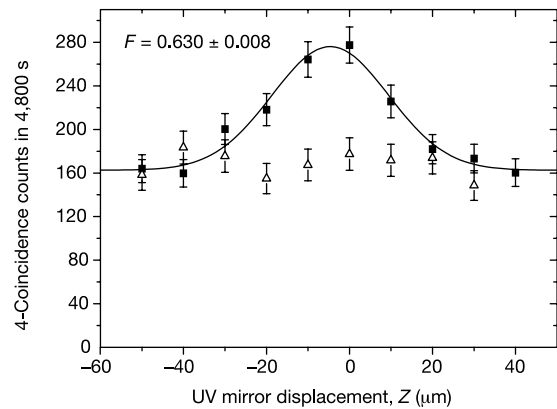


Figure 5 Experimental verification of the optimum conditions of the U-NOT gate. The height of the central peak expresses the rate measured with the π -analyser of mode \mathbf{k}_2 set to measure the ‘correct’ vertical (V) polarization, that is, the one orthogonal to the (H) polarization of the input π -state, $|\Psi\rangle = |H\rangle$ of the injected single photon, $N = 1$. By turning by 90° the π -analyser, the amount of the ‘noise’ contribution is represented by a ‘flat’ curve. The noise contribution is provided by the amplification of the unavoidable QED vacuum field on the input mode \mathbf{k}_1 . Filled squares, plots corresponding to the ‘correct’ polarization; open triangles, plots corresponding to the ‘noise’. The solid line represents the best gaussian fit to the results expressing the ‘correct’ polarization.

cal value of $F = 2/3 = 0.666$. Note that the height of the central peak in Fig. 5 does not decrease towards zero for large values of Z , as expected. This effect, due to instrumental imperfections, is discussed in Methods.

By a different measurement configuration, the apparatus was adopted to investigate the process of ‘quantum cloning’ of an $N = 1$ input qubit into $M = 2$ output qubits on mode k_1 . We have confirmed the results of ref. 9 by attaining a cloning fidelity $F = 0.810 \pm 0.008$ (theoretical value, $F = 5/6 \approx 0.833$). □

Methods

Basic optical equipment

The main source of all experiments was a Ti:Sa coherent MIRA mode-locked pulsed laser, providing (by second harmonic generation, SHG) the ‘pump’ field for the quantum-injected OPA associated with the spatial mode having wavevector k_p and wavelength $\lambda_p = 397.5$ nm (that is, in the UV range of the spectrum⁶). The time duration of each UV pulse was $\tau \approx 140$ femtoseconds (fs). The OPA active element, consisting of a 1.5-mm-thick NL crystal of β -barium borate (BBO) cut for type II phase-matching, was able to generate by SPDC—that is, by amplification of the vacuum field—linear polarization (π)-entangled pairs of photons. The ‘intrinsic phase’ of the OPA was set so as to generate by SPDC ‘singlet’ entangled states on the output optical modes, k_1, k_2 (ref. 10). The photons of each pair were emitted with equal wavelengths $\lambda = 795$ nm over two spatial modes k_1 and k_2 making an external angle of 8° . In all experiments, the time (t) optical walk-off effects due to the birefringence of the NL crystal were compensated by inserting in the modes k_1 and k_2 fixed X-cut, 4.8-mm-thick quartz plates (Figs 2 and 4). All adopted photodetectors (D), but D_2 , were equal SPCM-AQR14 Si-avalanche nonlinear single-photon units with nearly equal quantum efficiencies ~ 0.55 . One interference filter with bandwidth $\Delta\lambda = 6$ nm was placed in front of each detector D. Only the detector D_2 (Fig. 2) was a linear photodiode. Polarizing beam-splitters (PBS) in Figs 2 and 4 are adopted from measurement devices providing polarization analysis.

Universality test

See Figs 2 and 3. Because the universality (U) of the OPA transformation (that is, the insensitivity of g to the (unknown) π state of any input photon) is a macroscopic ‘classical’ property of the OPA device, the U-test has been carried out by injection of the strongly attenuated laser beam, with wavelength $\lambda = 795$ nm, contributed via a beam splitter by the main mode-locked source and directed along the OPA injection mode k_1 . The parametric amplification, with $g \approx 0.11$, was detected at the OPA output mode k_2 by the linear Si photodiode SGD100 (D_2), filtered by an interference filter with bandwidth $\Delta\lambda = 3$ nm. The time superposition in the NL crystal of the ‘pump’ and of the ‘injection’ pulses was assured by micrometric displacements (Z) of a two-mirror optical ‘trombone’. The pulse shapes shown by the coincidence data (Figs 3 and 5) as function of Z are indeed the signature for actual amplification: that is, they arise from the effective time and space superposition in the NL crystal of the UV ‘pump’ pulse and of the optical pulses with $\lambda = 795$ nm, injected into the OPA. Relevant, different π -states of the injected field, formally expressed by the captions of the panels of Fig. 3, were prepared by a single wave-plate WP_1 , corresponding to a suitable optical retardation, equal to $\lambda/2$ or to $\lambda/4$, between the two orthogonal basis π -states, that is, horizontal (H) and vertical (V). The OPA amplified output π -states were detected by an apparatus inserted on mode k_2 and consisting of the set ($WP_2 + \pi$ -analyser), the last device being provided by the polarizing beam splitter PBS_2 .

Realization of the U-NOT gate

See Figs 4 and 5. The UV pump beam, back-reflected by a spherical mirror M_p with 100% reflectivity and micrometrically adjustable-position Z , excited the NL OPA crystal amplifier in both directions ($-k_p$) and k_p , correspondingly oriented towards the right (R) and the left (L) sides of Fig. 4. An SPDC process excited by the $-k_p$ pump mode created single photon-pairs with wavelength $\lambda = 795$ nm in entangled singlet π -states. One photon of each pair, emitted over $-k_1$, was reflected by a spherical mirror M onto the NL crystal where it provided the $N = 1$ quantum injection into the OPA excited by the UV pump beam associated with the back-reflected mode k_p . Consider the qubit flipping related to the OPA injection of a single photon ($N = 1$) over the mode k_1 in the state $|\Psi\rangle = |H\rangle$. Because of the low pump intensity, the $N = 2$ photon injection probability has been evaluated to be $\sim 10^{-2}$ smaller than the one for $N = 1$. The twin photon emitted over $-k_2, \pi$ -selected by the devices ($WP_2 + PBS_2$) and detected by D_2 , provided the ‘trigger’ of the overall experiment. Because of the EPR non-locality implied by the singlet state, the π -selection on mode $-k_2$ provided the realization on k_1 of the state $|\Psi\rangle = |H\rangle$ of the injected photon. The field’s π -state on the output mode k_2 was analysed by the optical device combination ($WP_2^* + PBS_2^*$) and measured by D_2^* . Detectors D_a, D_b were coupled to the field associated with the mode k_1 via a normal beam splitter, BS. The rate of the four-coincidences involving all detectors (D_2^*, D_2, D_a, D_b) was experimentally measured by an electronic four-coincidence apparatus having a time resolution of 3 ns. Note that the height of the central peak in Fig. 5 does not decrease towards zero for large values of $|Z|$, as expected. This effect is attributable entirely to the limited time resolution of the four-coincidence apparatus. The effect would disappear if the resolution could be pushed into the sub-picosecond range, precisely of the order of the time duration of the interacting pump and injection pulses: $\tau' \approx 140$ fs. Such a resolution is hardly obtainable with the present technology.

Received 31 May; accepted 23 August 2002; doi:10.1038/nature01093.

1. Bechmann-Pasquinucci, H. & Gisin, N. Incoherent and coherent eavesdropping in the six-state protocol of quantum cryptography. *Phys. Rev. A* **59**, 4238–4248 (1999).
2. Bužek, V., Hillery, M. & Werner, R. F. Optimal manipulations with qubits: Universal-NOT gate. *Phys. Rev. A* **60**, R2626–R2629 (1999).
3. Gisin, N. & Popescu, S. Spin flips and quantum information for antiparallel spins. *Phys. Rev. Lett.* **83**, 432–435 (1999).
4. Alber, G. et al. *Quantum Information: An Introduction to Basic Theoretical Concepts* (Springer Tracts in Modern Physics Vol. 173, Springer, Berlin, 2001).
5. Derka, R., Bužek, V. & Ekert, A. K. Universal algorithm for optimal estimation from finite ensembles via realizable generalized measurement. *Phys. Rev. Lett.* **80**, 1571–1575 (1998).
6. De Martini, F. Amplification of quantum entanglement. *Phys. Rev. Lett.* **81**, 2842–2845 (1998).
7. Simon, C., Weihs, G. & Zeilinger, A. Optimal quantum cloning by stimulated emission. *Phys. Rev. Lett.* **84**, 2993–2996 (2000).
8. De Martini, F., Mussi, V. & Bovino, F. Schroedinger cat states and optimal universal quantum cloning by parametric amplification. *Opt. Commun.* **179**, 581–589 (2000).
9. Lamas-Linares, A., Simon, C., Howell, J. C. & Bouwmeester, D. Experimental quantum cloning of single photons. *Science* **296**, 712–714 (2002).
10. De Martini, F., Di Giuseppe, G. & Padua, S. Multiparticle quantum superpositions and stimulated entanglement by parity selective amplification of entangled states. *Phys. Rev. Lett.* **87**, 150401 (2001).

Acknowledgements We thank M. Hillery, C. Simon, S. Popescu, M. D’Ariano for discussions, and V. Mussi, A. Mazzei, F. Bovino, S. Padua for early experimental collaboration. This work was supported by the FET European Networks ATEST, EQUIP, QUBITS, MURST, and INFN.

Competing interests statement The authors declare that they have no competing financial interests.

Correspondence and requests for materials should be addressed to F.D.M. (e-mail: francesco.demartini@uniroma1.it).

Observation of coupled magnetic and electric domains

M. Fiebig*†, Th. Lottermoser*, D. Fröhlich*, A. V. Goltsev‡ & R. V. Pisarev‡

* Institut für Physik, Universität Dortmund, 44221 Dortmund, Germany

† Max-Born-Institut, Max-Born-Straße 2A, 12489 Berlin, Germany

‡ Lofte Physical Technical Institute of the Russian Academy of Sciences, 194021 St Petersburg, Russia

Ferroelectromagnets are an interesting group of compounds that complement purely (anti-)ferroelectric or (anti-)ferromagnetic materials—they display simultaneous electric and magnetic order^{1–3}. With this coexistence they supplement materials in which magnetization can be induced by an electric field and electrical polarization by a magnetic field, a property which is termed the magnetoelectric effect⁴. Aside from its fundamental importance, the mutual control of electric and magnetic properties is of significant interest for applications in magnetic storage media and ‘spintronics’^{2,3}. The coupled electric and magnetic ordering in ferroelectromagnets is accompanied by the formation of domains and domain walls. However, such a cross-correlation between magnetic and electric domains has so far not been observed. Here we report spatial maps of coupled antiferromagnetic and ferroelectric domains in $YMnO_3$, obtained by imaging with optical second harmonic generation. The coupling originates from an interaction between magnetic and electric domain walls, which leads to a configuration that is dominated by the ferroelectromagnetic product of the order parameters.

The ferroelectromagnetic (FEM) manganites $RMnO_3$ with $R \in \{Sc, Y, In, Ho-Lu\}$ are multiple-order-parameter compounds with four 180° domains denoted by $(+P, +I)$, $(+P, -I)$, $(-P, +I)$, $(-P, -I)$ ⁵. Here, $\pm P$ is the independent component of the ferroelectric (FEL) order parameter, a polar vector, which is invariant under time reversal⁶ and describes the breaking of the inversion symmetry due to the FEL polarization along the hexagonal z axis below the Curie temperature $T_C = 570\text{--}990$ K⁷. On the other hand,